ISSN 2176-5480

22nd International Congress of Mechanical Engineering (COBEM 2013)
November 3-7, 2013, Ribeirão Preto, SP, Brazil

NUMERICAL SIMULATION OF A BITUMINOUS COAL PARTICLE COMBUSTION IN O_2/N_2 AND O_2/CO_2 ATMOSPHERES

Juan Esteban García Sierra
Fábio Alfaia da Cunha
University of Brasilia, Brazil
jgarcias8832@gmail.com; fabioalfaia@unb.br

Carlos Alberto Gurgel Veras
University of Brasilia, Brazil
gurgel@unb.br

Abstract. *Confirming the predictions about large oil and natural gas reserves depletion, coal may once again become a major source of fossil fuel in the world. The large-scale use of coal will probably be associated with techniques for capturing and storing carbon dioxide. The combustion in O_2/CO_2 atmosphere (Oxy-fuel combustion), is currently one of the principal technological options being considered for capturing carbon dioxide from coal combustion. This paper presents a detailed study of the combustion of a single axisymmetric coal particle in O_2/N_2 and O_2/CO_2 atmospheres. The prediction of coal combustion was done through numerical simulation. Conservation equations for mass, species, energy and momentum are solved numerically by a control volume finite element method (for a two-dimensional axisymmetric geometry). The particle was considered as a porous material that can change due to pyrolysis, combustion and gasification processes. This paper shows the combustion time, concentration and temperature profiles. All of this is done for different concentrations of O_2 in the O_2/CO_2 mixture.*

Keywords: *oxy-fuel, combustion, numerical simulation, bituminous coal, CO_2 capture.*

1. INTRODUCTION

Energy production from fossil fuels combustion contributes to the emission of greenhouse gases, which dominant provider is the CO_2. Public awareness and legislation have led to policies to reduce emissions of greenhouse gases in the economically well-developed countries with initiatives and regulations as the Kyoto Protocol and the Intergovernmental Panel on Climate Change (IPCC, 2004). During the last decades, the role of coal as an energy source has remained steady due to its vast availability, stability and cost. However, coal emits more CO_2 into the atmosphere than any other fuel. Therefore, recently there has been developing research on new processes for the production of electricity from coal combustion through technologies that minimize environmental impact (Ziemniczac and da Silva, 2012). Technologies being developed for CO_2 capture and sequestration from combustion and gasification technologies include (IEA, 2005): post-combustion, pre-combustion, oxy-fuel combustion and chemical looping. After capture and compression, CO_2 must be transported and stored safely in suitable geological formations. The transportation is performed by ship or by pipeline, which are generally the cheapest forms of transport. The geological storage can be done mainly in saline aquifers, oil and gas fields and coal seams (CEPAC, 2008).

This review covers the oxy-fuel combustion option. This technology is presented as an excellent alternative for obtaining energy with real possibilities for reducing emissions of pollutants into the atmosphere. The coal combustion with pure oxygen produces a gas rich on CO_2 and water vapor, with substantially lower concentrations of NOx, allowing easy separation and capture of CO_2 which can then be compressed, transported and stored. Part of the rich gas in CO_2 is recirculated to control flame temperature and make up the volume of the missing N_2 to ensure there is enough gas to carry the heat through the boiler (Buhre et al., 2005). The high oxygen demand is provided by a cryogenic air separation process, which is currently the most mature and commercially evaluated technology (Scheffknecht et al., 2011).

The concept of oxy-fuel combustion was proposed in 1982 by Abraham (Abraham et al., 1982) in the context of providing a CO_2-rich fuel gas for enhanced oil recovery. There are many reviews of the development of this technology in the literature (Kiga, 2001; White et al., 2003; Wall, 2005; Croiset et al., 2005; Allam et al., 2005; Buhre et al., 2005; Santos et al., 2006; Wall et al., 2009; Scheffknecht et al., 2011). Oxy-fuel combustion technology is currently undergoing rapid development towards commercialization with a number of demonstration projects such Wall and Yu (2009), Hjärstman et al. (2009), Nikolopoulos et al. (2011) and Abbas et al. (2011), provided a comprehensive overview on the most recent developments in pilot plants and demonstration projects worldwide for the oxy-fuel technology. There are a number of pilot-scale facilities around the world, typically ranging in size from about 0.3–3.0MWth. However, Spain comes to the forefront of the technology with the CO_2 *compostilla's* project. Currently it has a Circulating Fluidized Bed (CFB) boiler of 30 MWth, capable of operating on air mode (as in the current thermal plants) and oxy-fuel mode. This boiler has been designed, and manufactured by Foster Wheeler SL from Spain and is funded

ISSN 2176-5480

by the Economic Recovery Energy Programme of the European Union. CIUDEN, Endesa and Foster Wheeler Oy cooperate in this project, aimed at validating CFB oxy-fuel technology and further developmening it into a second phase to build an industrial sized plant of 300MWe (OXYCFB300, 2012).

For the construction of new thermal plants based in oxy-fuel coal combustion technology or the adaptation of this technology on existing plants, it is necessary to continue searching and analyzing data and estimates that ensure the correct running and efficiency of the large-scale use of coal combustion based on oxy-fuel combustion. In this sense, computational numerical studies to evaluate this technology are still necessary. The model appears as a suitable alternative to methodological studies in the search of data and estimates for future developments to aid in the construction of power generation plants based in oxy-fuel combustion technology. Within this context, this paper aims to present a detailed study of the combustion of northern Colombian bituminous coal particle in O_2/NO_2 and O_2/CO_2 atmospheres through computational numerical simulations. The effect of replacing N_2 by CO_2 in the processes is presented. A spherical particle and different concentrations of O_2 in the O_2/CO_2 mixture were studied. The numerical simulations were performed on the computational fluid dynamics code developed in Cunha (2010).

2. MODELING OF COMBUSTION

2.1 Pyrolysis model

To model the rate of devolatilization of coal particles, the Correlation of the pyrolysis kinetics with a single Arrhenius type rate expression was considered assuming first order behavior with respect to volatile matter remaining in the char (Borman and Ragland, 1998):

$$\dot{\omega}_{pyr} = \frac{d\rho_v}{dt} = \rho_v k_{pyr} \tag{1}$$

Where $\rho_v = \rho_p - \rho_c - \rho_a$ (i.e. the density of the volatiles equals the density of the dry particle minus the density of the char and ash) and $k_{pyr} = -k_{0,pyr} \exp\left[-E_{pyr}/\left(\hat{R}T_p\right)\right]$. For a bituminous coal: the frequency factor is $k_{0,pyr} = 700\ s^{-1}$ and the energy activation is $E_{pyr} = 11.3\ kcal/gmol$.

Carbonic material is only available for heterogeneous reactions, according as the solid fuel is thermally degrades emitting volatile and forming the carbonic residue: $m_{cs} \xrightarrow{pyrolysis} m_v + m_c$. Table 1 presents the composition of volatile gases (m_v), calculated based on the work of Thunman et al. (2001) and applied to coal.

Table 1. Gas composition produced during devolatilization

Components	H_2	CO	CO_2	H_2O	CH_4	C_6H_6
Mass fraction (f_{pi})	0.09	0.26	0.10	0.14	0.04	0.37

2.2 Mechanisms for heterogeneous reactions

The combustion of solids presents a heterogeneous reaction, which according to Turns (2000) are those involving chemical species in different physical states. The heterogeneous reactions considered were char oxidation with O_2 and char gasification with CO_2. They are represented by reactions R1 and R2, respectively, (Ulzama, 2007), as show in tab. 2.

Table 2. Global mechanisms for heterogeneous reactions

	Reactions	heterogeneous reaction rates for coal (kmol/m^{2}s)
R1	$V_{C,C-O_2}C+O_2 \rightarrow 2(V_{C,C-O_2}\text{-}1)\,CO+(2-V_{C,C-O_2})\,CO_2$	$\hat{R}_{C-O_2} = 7x10^5\ e^{-1.6x10^5/RT}\ C_{O_2}$
R2	$C+CO_2 \rightarrow 2CO$	$\hat{R}_{C-CO_2} = 3.5x10^5\ e^{-2.2x10^5/RT}\ C_{CO_2}$

In reaction R1, the CO and CO_2 were recognized as primary products. For coal, the product ratio of CO /CO_2, named η, was related through the relationship of Tognotti et al. (1990): $\eta = 70e^{-3070/T_s}$. The stoichiometric carbon was calculated as: $\nu_{C,C\text{-}O_2} = 2\left(\frac{\eta+1}{\eta+2}\right)$.

ISSN 2176-5480

2.3 Mechanisms for homogeneous reactions

The mechanisms for homogeneous reactions are presented in Tab. 2 and tab. 3. Only eleven species were considered in the simulations: H, H_2, OH, H_2O, HO_2, O, O_2, CO, CO_2, CH_4, C_6H_6. CH_4 represents the light hydrocarbon and C_6H_6 is the tar. The partial oxidation of CH_4 and C_6H_6 are presented by reactions R3 and R4, respectively, given the constants rates by Westbrook and Dryer (1984) in tab. 3. The reactions from R5 to R14, represent the total oxidation of CO and H_2, given the rates constants by Warnatz et al. (2006) in tab. 4.

Table 3. Global mechanisms for partial oxidation of CH_4 and C_6H_6.

	Reactions	Expression Rate
R3	$CH_4+\frac{1}{2}O_2\leftrightarrow CO+2H_2$	$\hat{R}_{CH_4}= 4x10^9 e^{(-24.4x10^3/T)}[CH_4]^{-0.3}[O_2]^{1.3}$
R4	$C_6H_6+3O_2\rightarrow 6CO+3H_2$	$\hat{R}_{C_6H_6}= 2.31x10^9 e^{(-1.00x10^3/T)}[C_6H_6]^{-0.1}[O_2]^{1.85}$

Units are kmol, s, m^3, J, and K.

Table 4. Skeletal mechanism for CO and H_2 reactions.

Rate coefficients in Arrhenius form: $k_f = AT^n exp(-E/RT)$				
	Reactions	A	E	n
R5	$OH+OH\leftrightarrow O+H_2O$	3.57×10^1	-8.83×10^6	2.4
R6	$CO+OH\leftrightarrow CO_2+H$	1.00×10^{10}	66.9×10^6	0
	$k_f = A_1T^{n1}exp(-E_1/RT)+A_2T^{n2}exp(-E_2/RT)+A_3T^{n3}exp(-E_3/RT)$	1.01×10^8	0.25×10^6	0
		9.03×10^8	19.1×10^6	0
R7	$H+O_2\leftrightarrow OH+O$	2.07×10^{11}	62.9×10^6	-0.097
R8	$O+H_2\leftrightarrow OH+H$	3.82×10^9	33.3×10^9	0
	$k_f = A_1T^{n1}exp(-E_1/RT)+A_2T^{n2}exp(-E_2/RT)$	1.0310^{12}	80.2×10^6	0
R9	$OH+H_2\leftrightarrow H_2O+H$	2.17×10^5	14.5×10^6	1.52
R10	$H+OH+M\rightarrow H_2O+M$	2.20×10^{16}	0	-2
R11	$H+O_2+M\rightarrow HO_2+M$	2.8×10^{12}	0	-0.86
R12	$H+HO_2\rightarrow OH+OH$	4.46×10^{11}	5.82×10^6	0
R13	$H+HO_2\rightarrow H_2+O_2$	1.05×10^{11}	8.56×10^6	0
R14	$OH+HO_2\rightarrow H_2O+O_2$	9.28×10^{12}	73.3×10^6	0

Units are kmol, s, m^3, J, and K.

2.4 Average Conservaion's equations in volume

2.4.1 Conservation equations for mass and momentum, for incompressible flow and Newtonian fluids, can be written as (Whitaker, 2005):

$$\frac{\partial}{\partial t}\left(\varepsilon\rho\right)+\nabla\cdot\left(\rho\mathbf{u}\right)=\dot{\omega}_{pyr}+\Sigma_{k=1}^{n_{R,S}}\dot{\omega}_{s,k} \tag{2}$$

$$\frac{\partial}{\partial t}\left(\frac{\rho\mathbf{u}}{\varepsilon}\right)+\nabla\cdot\left(\frac{\rho\mathbf{u}\mathbf{u}}{\varepsilon^2}\right)=-\nabla p+\rho\mathbf{g}+\nabla\cdot\left(\frac{\mu_e\nabla\mathbf{u}}{\varepsilon}\right)+\left(\nabla p\right)_p \tag{3}$$

The term $\dot{\omega}_{pyr}$ represents a source of mass due to degradation of the solid and $\Sigma_{k=1}^{n_{R,S}}\dot{\omega}_{s,k}$ represents a source of mass due heterogeneous reactions. The term $\left(\nabla p\right)_p=-\frac{\mu g}{K}\mathbf{u}-C_F\frac{\rho}{\sqrt{K}\varepsilon^{3/2}}|\mathbf{u}|\mathbf{u}$ represents the drag force applied by the solid phase.

2.4.2 Conservation equation for energy (Viskanta, 2005):

$$\frac{\partial}{\partial t}\left(\varepsilon\rho c_p T_g\right)+\nabla\cdot\left(\rho c_p\mathbf{u}T_g\right)=\nabla\cdot\left(k\nabla T_g\right)+S_{T,g} \tag{4}$$

Where thermal properties of the energy equation, are calculated as follows

$$\rho c_p=\left(1-\varepsilon+\right)\rho_{s,1}c_{p,s}+\varepsilon\rho_g c_{p,g} \tag{5}$$

ISSN 2176-5480

$$k = (1-\varepsilon)k_s + \varepsilon k_g + k_{rad} \tag{6}$$

Where $c_{p,g}$ and k_g are specific heat and thermal conductivity of the gaseous material. $c_{p,s}$ and k_s are specific heat and thermal conductivity of the solid material. $\rho_{s,I}$ is the intrinsic density of the solid material. The effect of radiative heat transfer was incorporated by raising the conductivity k_{rad}.

Source term of the energy equation is given as:

$$S_{T,g} = -\varepsilon\Sigma_{k=1}^{n_{esp}}\dot{\omega}_{g,k}h_k + Q_{rad} + \dot{\omega}_{pyr}H_{pyr} + \Sigma_{k=1}^{n_{R,S}}\dot{\omega}_{s,k}H_k \tag{7}$$

The term $\Sigma_{k=1}^{n_{esp}}\dot{\omega}_{g,k}h_k$ represents the heat generation due to chemical reactions (homogeneous). As for the terms $\dot{\omega}_{pyr}$ and $\dot{\omega}_{s,k}$ represent the mass conversion rates due to pyrolysis and heterogeneous reactions, respectively. H_{pyr} is the heat of reaction due to pyrolysis and H_i is the heat of reaction due to heterogeneous reactions. The term $Q_{rad} = A_{sur}\sigma\varepsilon_{rad}\left(T_{rad}^4 - T_s^4\right)$ represents radiative power exchanged in the environment, assumed to a reference temperature T_{rad}, and the porous medium. This exchange takes place across the interface between means, so it only provides power to the nodes located in this position. A_{sur} is the surface area involving the particle (m^2) and the parameters σ and ε_{rad} are the Stefan-Boltzmann constant (W/m^2K^4) and radiative emissivity of the particle, respectively.

2.4.3 Conservation equation for chemical species (Viskanta, 2005):

$$\frac{\partial}{\partial t}(\varepsilon\rho Y_k) + \nabla\cdot(\rho\mathbf{u}Y_k) = \nabla\cdot(\varepsilon\mathbf{J}_k) + \dot{\omega}_{g,k} + \dot{\omega}_{s,k} + f_{p,k}\dot{\omega}_{pyr},\ k = 1, 2, \ldots, \mathrm{N_{sp}} \tag{8}$$

Where N_{sp} is the total number of gaseous chemical species present in the system. Fick's Law is used to approximate the diffusion: $\mathbf{J}_k = -\rho D_{k,eff}\nabla Y_k + Y_k\mathbf{J}_c$, and $\mathbf{J}_c = -\sum_{k=1}^{N_{sp}}\left(-\rho D_{k,eff}\nabla Y_k\right)$ is a correction, similar to that proposed by Curtiss-Hirschfelder (1949). The term $\dot{\omega}_{g,k}$ is the net rate of production of the species k by chemical reaction and $\dot{\omega}_{s,k}$ represents the net rate of production of the species k due to degradation of the solid.

2.5 Thermo-physical properties

The ideal gas model is used to relate the density of the gas mixture with the temperature:

$$\rho = (p\overline{W})/(RT) \tag{9}$$

The molecular weight of the mixture gases is obtained from the composition of the gases: $\overline{W} = \left(\Sigma_{k=1}^{N} Y_k/W_k\right)^{-1}$, where Y_k and W_k are the mass fraction and molecular weight of a given species k respectively.

The specific heat of the gas mixture at constant pressure can be obtained as:

$$c_{p,g} = \Sigma_{k=1}^{Nsp} Y_k c_{p,k} \tag{10}$$

The specific heat of the single species —k is calculated as a function of temperature.

$$c_{p,k} = aT + bT^2 + cT^3 + dT^4 \tag{11}$$

The constants were taken from Turns (2004).

ISSN 2176-5480

Viscosity and thermal conductivity of the gas mixture are calculated based on the pure components of the mixture (Bird et al. 2001):

$$\mu = \sum_{k=1}^{Nsp} \frac{Y_k \mu_k}{\sum_{j=1}^{Nsp} Y_j \Theta_{kj}} \tag{12}$$

$$k = \sum_{k=1}^{Nsp} \frac{Y_k k_k}{\sum_{j=1}^{Nsp} Y_j \Theta_{kj}} \tag{13}$$

The viscosity, thermal conductivity and Θ_{kj} were calculated from expressions obtained from Bird et al. (2001).

Bulk and Knudsen diffusion may contribute to the mass transport within the porous structure. The combined effect of the two diffusion mechanisms described can be condensed in an effective diffusion coefficient, $D_{k.eff}$ expressed as:

$$1/D_{k.eff} = (\tau/\varepsilon)(1/D_{km} + 1/D_{K,k}) \tag{14}$$

Where: D_{km} represents the *bulk* diffusion coefficient of the species k and $D_{K,k}$ is the Knudsen diffusion coefficient.

Bulk diffusion coefficient of the component k in the mixture may be calculated as follows (Turns, 2000):

$$D_{km} = (1 - X_k)\left[\sum_{\substack{j=2 \\ j\neq}}^{N_{sp}} \frac{X_j}{D_{kj}}\right]^{-1} \tag{15}$$

Binary diffusivity, D_{kj}, is calculated using the Chapman-Enskog equation (see Bird et al., 2001).

Thermal conductivity of the solid material is calculated as:

$$k_s = \eta_{sf} k_{sf} + \eta_{ash} k_{ash} \tag{16}$$

Where k_{sf} and k_{ash} are the solid fuel and ash conductivities, respectively. m_s, m_{sf} and m_{ash} are the mass of solid, mass of fuel solid and mass of ash, respectively. Additionally $\eta_{sf} = m_{sf}/m_s$, $\eta_{ash} = m_{ash}/m_s$ and $k_{ash} = 6.18 \times 10^{-4} T + 1.2$.

Conductivity of the solid fuel was calculated from the equation proposed by Atkinson and Merrick (1982):

$$k_{sf} = (\rho_{s,I}/4511)^{3.5} T^{0.5} \tag{17}$$

Radiative conductivity is defined as:

$$k_{rad} = 4\sigma \varepsilon_{rad} d_p T_s^3 \tag{18}$$

Where σ is the Stefan-Boltzmann constant, d_p is the size of largest pores.

Specific heat of the solid, considering the ash effect, is accounted for:

$$c_{p,s} = \eta_{sf} c_{p,sf} + \eta_{ash} c_{p,ash} \tag{19}$$

Where $c_{p,s}$ and $c_{p,ash}$ are the specific heats of the solid fuel and ash, respectively. These specific heats are calculated from the equations $c_{p,ash} = 593.3 + 0.586 T_s$

The specific heat of the solid fuel, in dry basis and free of ash, was calculated with the equation proposed by Merrick (1982):

$$c_{p,sf} = (Ru/\bar{W}_s)[g_1(380/T_s^{-1}) + 2g_1(1800/T_s^{-1})] \tag{20}$$

ISSN 2176-5480

Where $g_1(X)=\left(X^2e^X\right)\left(e^X-1\right)^{-2}$ and the parameter $\overline{W}_s$ represents the average atomic weight of the solid.

Permeability is calculated as a function of pore diameter (d_p) and porosity (ε) as (Krishna and Wesselingh 1997):

$$K=\left(d_p{}^2/180\right)\left(\varepsilon^2/(1-\varepsilon)^2\right) \tag{21}$$

2.6 Porous structure of the solid

A coal particle can be considered as a porous structure with different sizes and shapes of internal channels. Only a part of a porous structure is solid. The fraction of void volume in a solid is called porosity and is defined as:

$$\varepsilon \equiv V_g/V_T \tag{22}$$

Where: V_g is the void volume that can be occupied by gas in the porous structure and V_T is the total volume (solid volume + void volume).

The volume fraction of solid material $(1-\varepsilon)$ can be divided between solid components: volume fractions of ash, solid fuel and coke, respectively represented by X_{ash}, X_{sf}, X_c. Thus $(1-\varepsilon)=X_{ash}+X_{sf}+X_c$, that is, the porosity can be calculated from the volume fractions of the solid constituents. And the volume fractions can be calculated in terms of mass variation:

$$X_i=m_i/\left(\rho_{i,I}V_T\right) \tag{23}$$

Where *i* can be ash, solid fuel (sf), or carbonic materials (c). Thus it can be defined $\rho_{sf,I}$ as the intrinsic density of solid fuel (for bituminous coal ~ 1429kg/m^3), $\rho_{ash,I}$ is the intrinsic density of ash ~ 2260kg/m^3) and $\rho_{c,I}$ is the intrinsic density of coke (carbon residue formed by pyrolysis, approximately equal to the pure carbon ~ 2200kg/m^3). In the present work, $\rho_{ash,I}$, $\rho_{cs,I}$ and $\rho_{c,I}$ were assumed as invariant with the conversion of solid material.

The mass of each control volume that comprises the solid particle is calculated as:

$$m_s=\rho_{s,I}(1-\varepsilon)V_T=\underbrace{\rho_{sf,I}X_{sf}V_T}_{\text{mass of solidfuel}}+\underbrace{\rho_{c,I}X_cV_T}_{\text{mass of coke}}+\underbrace{\rho_{ash,I}X_{ash}V_T}_{\text{mass of ash}} \tag{24}$$

3. COMPOSITIONS

The fuel composition is of a northern Colombian bituminous coal. The proximate and ultimate analysis, surface area (Sa) and porosity (**ε**), were taken form Rojas and Barraza (2007) and are presented in Tab. 5.

Table 5. Properties of coal

Proximate analysis (% dry basis)			Ultimate analysis					Sa (m_2/g)	ε (%)
Volatiles	Char	Ash	% C	% H	% N	% S	% O	13.16	54.5
35.6	52.8	11.6	82.4	5.9	1.3	0.9	9.5		

4. NUMERICAL SOLUTION AND BOUNDARY CONDITIONS

The numerical simulations were performed on the computational fluid dynamics code developed in Cunha (2010). In such code, governing equations are solved using the control volume finite element method. The pressure-velocity coupling algorithm used was similar to Patankar's (1980) SIMPLE algorithm. A scheme of second order discretization was used in the discretization of the diffusive terms. The FLO scheme was used in the advective terms. The solver was adjusted to run the calculations with double precision.

ISSN 2176-5480

Geometry and Mesh

An axisymmetric coal particle was considered in the simulations. Figure 1 shows an overview of the model with the z-axis as the rotation axis. The domain dimensions were established based on simulations in order to minimize the contour effects on the results.

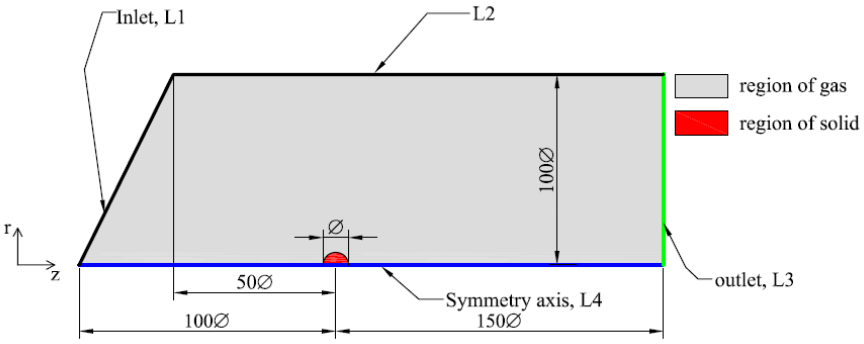

Figure 1 – Computational axisymmetric domain in cylindrical coordinates.

Boundary conditions and initial conditions for the combustion case are set out in Tab. 6.

Table 6 – Boundary conditions, BC, and initial conditions, IC.

IC	$t=0$	$\forall z \wedge \forall r$	$u=0$	$v=0$	$\phi=\phi_{initial}$
BC	L4	$\forall t$	$\partial u/\partial r=0$	$v=0$	$\partial \phi/\partial r=0$
BC	L2	$\forall t$	$u=u_{in}$	$v=0$	$\phi=\phi_{in}$
BC	L1	$\forall t$	$u=u_{in}$	$v=0$	$\phi=\phi_{in}$
BC	L3	$\forall t$	$\partial u/\partial z=0$	$\partial v/\partial z=0$	$\partial \phi/\partial z=0$

The mesh used in simulations is shown in fig. 2 (a). This mesh is composed of 892 nodes and 1669 elements. The solid medium is represented by 140 nodes. In some discrete mesh, nodal points are placed with porosity, permeability, density and thermo-physical properties of the solid. All these quantities change with the conversion. Figure 2 (b), shows the initial porosity field set to start the simulations.

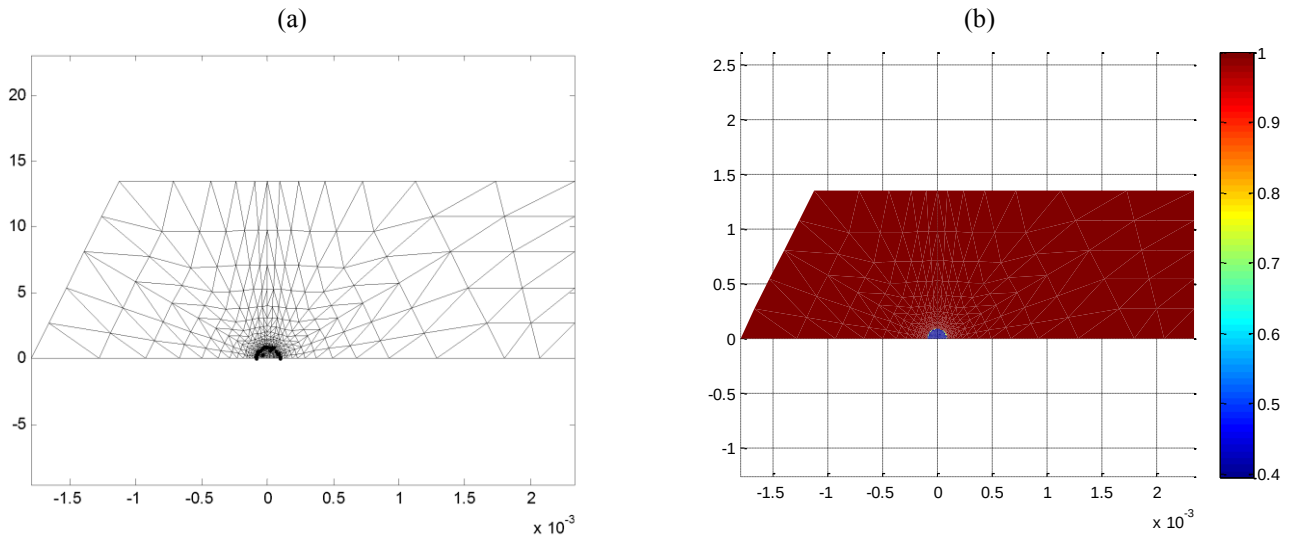

Figure 2 – (a) Mesh of finite elements and (b) example of initial porosity field.

ISSN 2176-5480

5. RESULTS AND DISCUSSIONS

In all our simulations was assumed that the particle was completely burnt when 99% of the combustible solid material had been consumed. The gas temperature was adjusted to 1400K equal to the input domain. The input rate was adjusted so that the Reynolds number (based on the particle diameter) was equal to 0.1. Different concentrations were adjusted in the input domain.

Figure 3, shows the burning time for different oxygen concentrations. In fig. 3, m_{sf} is solid fuel and $m_{sf,0}$ is solid fuel at initial time. The fraction $m_{sc}/m_{sc,0}$ should take values from one to zero. As expected, the burning time decreases with increasing oxygen concentration. Moreover, for equal concentrations of oxygen (in volume), the burning time in an O_2/N_2 atmosphere is less than in an O_2/CO_2 atmosphere. This occurs because the gasification reaction, which is endothermic, happens since the coke formation until the pyrolysis' end. Further, the O_2/CO_2 mixture is denser than O_2/N_2 mixture. Dissociation of CO_2 in the flame must also cooperate, absorbing heat and contributing to lessen the burning time.

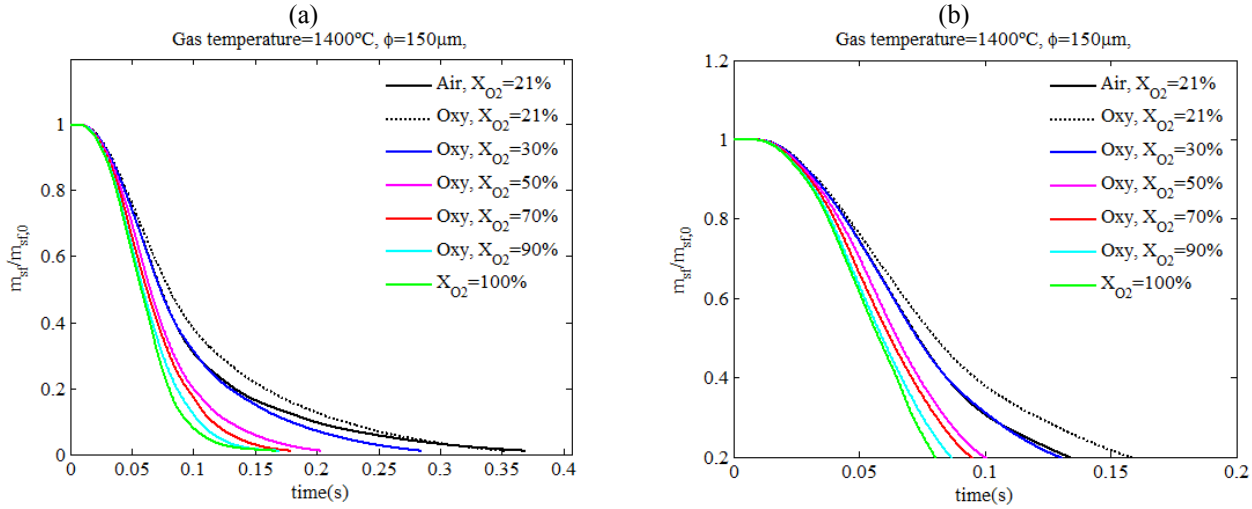

Figure 3 – weight loss: (a) 99% mass burning and (b) 80% mass burning

It was also observed that the combustion in pure oxygen environment is very fast (fig. 3), and the temperatures are too high (fig. 4). Therefore it is not possible to use pure O_2 to fuel combustion in equipments currently available in the industry. The aim is to dilute the oxygen with CO_2, so that the thermal behavior can be similar to coal combustion with atmospheric air (21% O_2 79% N_2). It has been reported in other studies that 30% O_2 and 70% CO_2 leads to a thermal behavior similar to conventional combustion with atmospheric air. The results depicted on fig. 4 (b) agree with such statement with respect to weight loss, equal to the results of Fig. 4 (a), where it can be observed that the maximum surface temperature of the particle burned with air, has a strong resemblance with the one that was burned in a mixture of 30% O_2 and 70% CO_2.

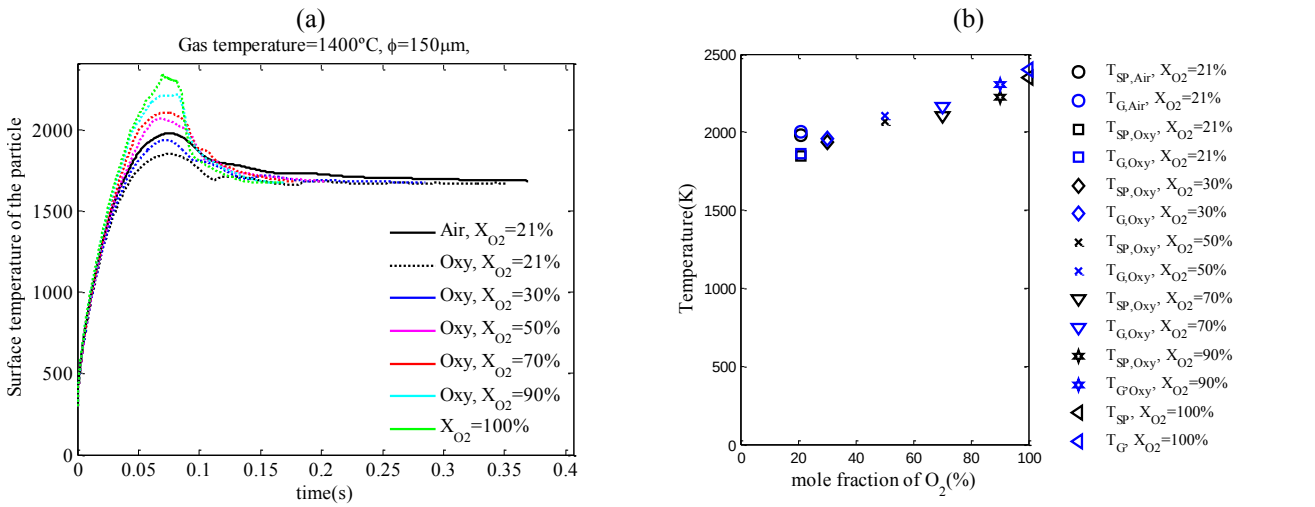

Figure 4 – (a) temperature of the particle and (b) maximum temperature: for particle=TSP and for gas=TG.

ISSN 2176-5480

In Figures 5 and 6 are shown species and temperature profiles in the region close to the particle in a time of 0.075 s. This time point was chosen because it marks the maximum temperatures.

It is seen in Figure 5 (a) that the oxygen concentration profiles are similar for air and oxy-fuel (21% O_2) conditions. Note that the concentration gradients are quite pronounced in the interior of the particle. Figure 5 (b) also shows a strong tendency within the particle, but in this case the CO_2 concentration profiles show a strong similarity between pure oxygen and the air case. This is due to low concentrations of CO_2 contained in atmospheric air.

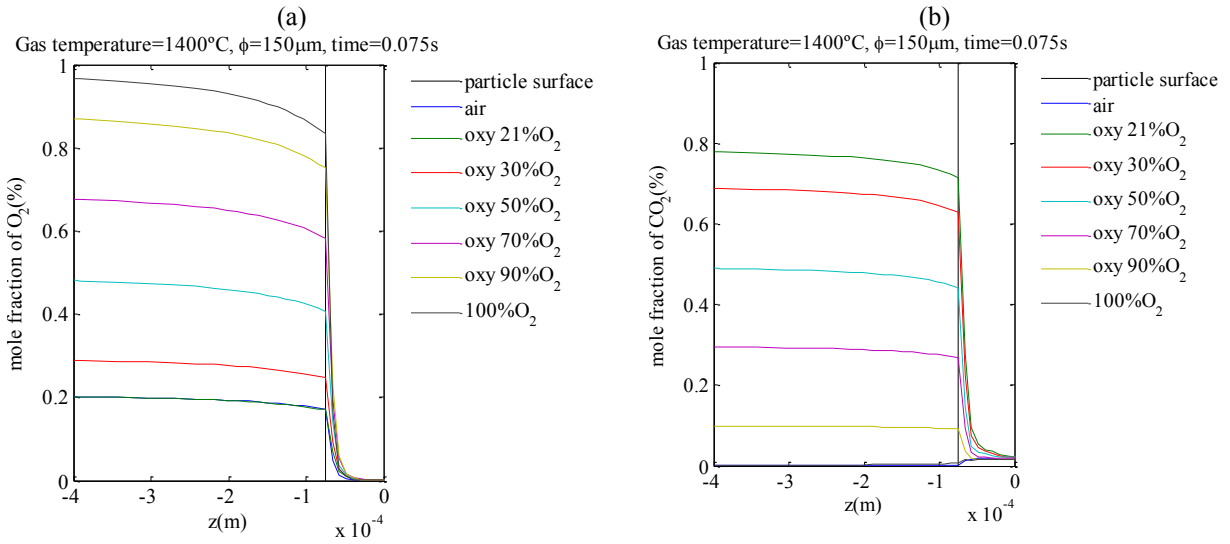

Figure 5 – mole fraction profiles near the particle for t=0.075s: (a) O_2 profile and (b) CO_2 profile

Concentration profiles of CO are similar for all concentrations under oxy-fuel conditions and pure oxygen, fig. 6 (a). As far as the CO mass fraction is concerned, under oxy-fuel conditions, the CO concentration in the flue gas is predicted to be higher than in atmospheric air conditions. This was confirmed experimentally by Tan et al. (2010), who claim that this is possibly due to the slower diffusion rate of volatiles under high CO_2 concentrations. In Figure 6 (b) it is observed that the temperature profile shows a very similar thermal behavior in the atmospheric air case compared with oxy-fuel (30% O_2 and 70% CO_2) case.

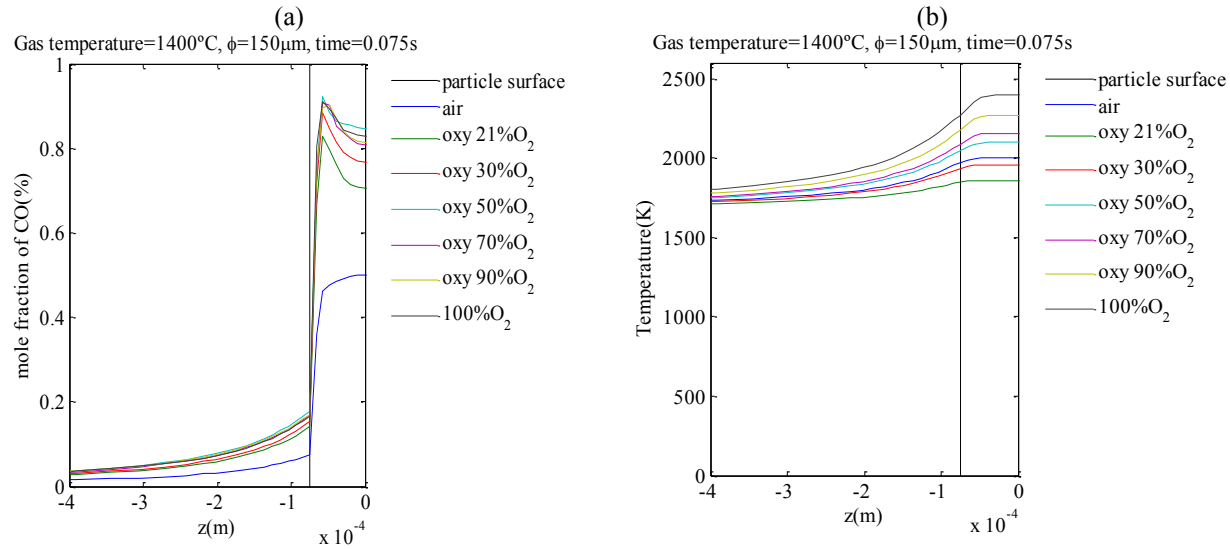

Figure 6 –profiles near the particle for t=0.075s: (a) profiles of CO and (b) Temperature profiles.

Figure 7, presents temperature fields for different values of $m_{sc}/m_{sc,0}$. For $m_{sc}/m_{sc,0}$=0.9 it is clearly perceptible a flame surrounding the particular. Insofar as $m_{sc}/m_{sc,0}$ reduces the maximum temperatures region, it passes into the interior of the particle.

Figure 8, shows the velocity field for two different instants for combustion with pure oxygen. The rate of entry into the domain is imposed as 0.17 m/s and the particle surface is marked by circular spots.

ISSN 2176-5480

In the first instant (t = 0.001 s), the flow only surrounds the particle and there is no flow inside the particle. In the second instant (t = 0.075 s), it is checked the gases formed inside the particle escaping at high speed. The maximum velocity at that time was 2.47 m/s, which is approximately 14 times the velocity of entry.

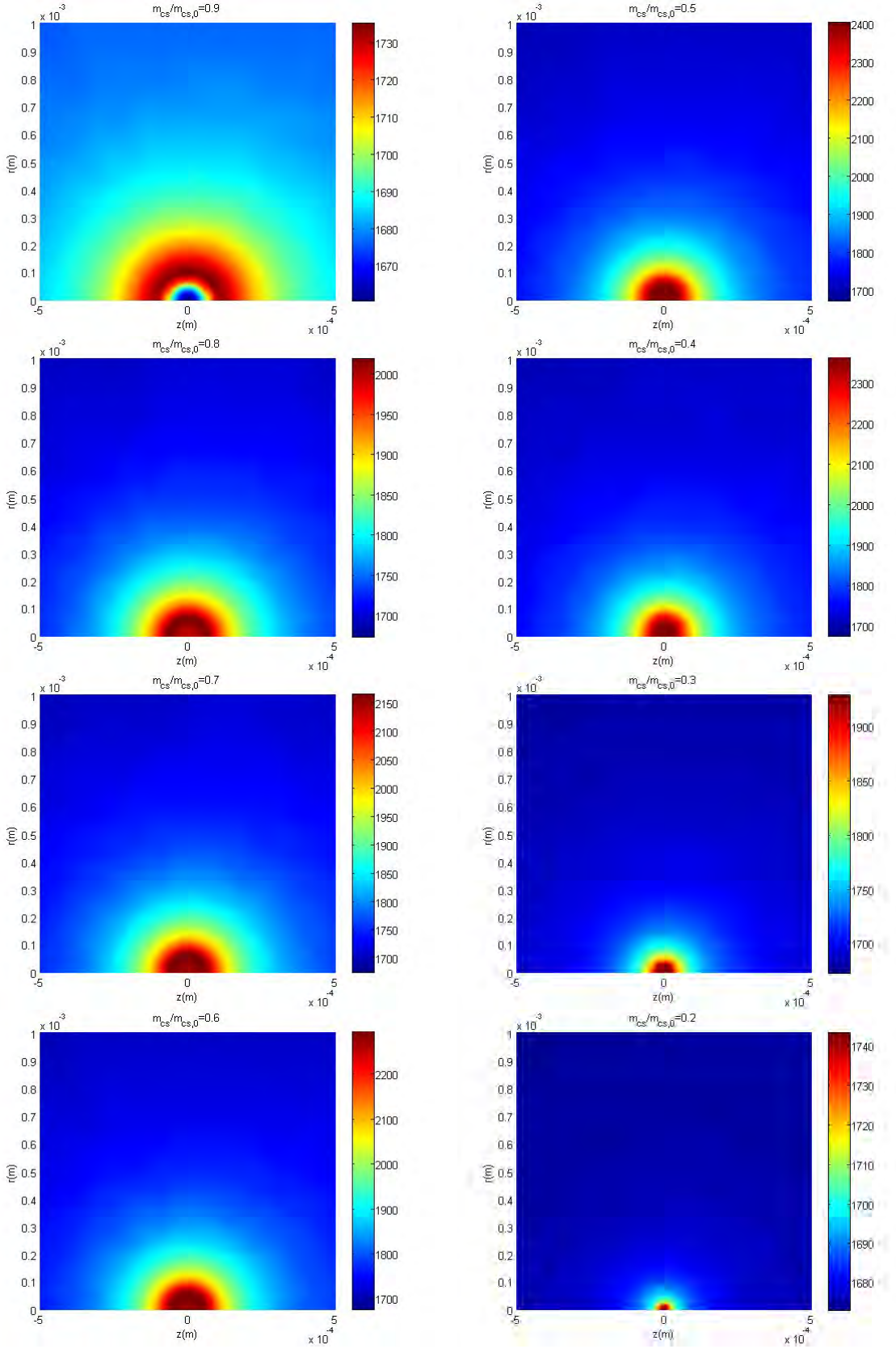

Figure 7 - Temperature field considering combustion in pure oxygen for different values of $m_{sc}/m_{sc,0}$,

ISSN 2176-5480

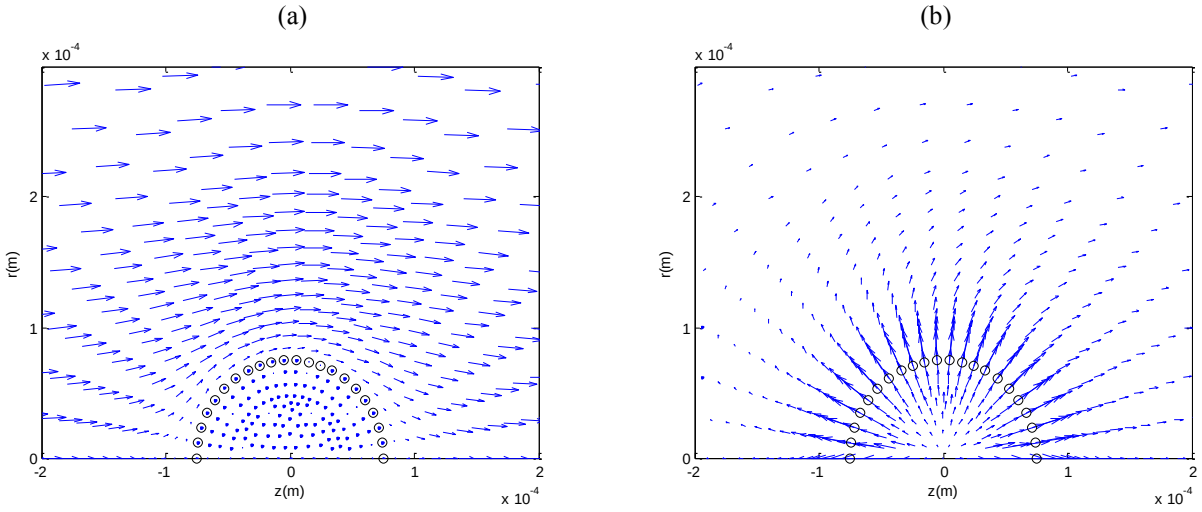

Figure 8 – velocity field: (a) t=0.001s and (b) t=0.075s.

6. CONCLUSIONS

A simulation model for combustion of axisymmetric coal particles was presented in this paper. The burning time, temperature and concentration of species profiles, for a northern Colombian coal particle with 0.150mm of diameter, were presented. Three totally different atmospheres were considered in the simulations: air, oxy-fuel and pure oxygen. It was found that oxy-fuel combustion with 30% of O_2 presents weight loss similar to the combustion air (21% O_2 and 79% N_2). The results presented are preliminary; it is expected to calibrate the numerical model for the northern Colombian coal, so that it can be developed in the near future damning statements about the processes that occur during combustion.

7. ACKNOWLEDGEMENTS

The authors gratefully acknowledged the ―Conselho Nacional de Desenvolvimento Científico e Tecnológico (CNPq)" for the financial support for the project: ―551317/2010-8 - Modelagem Numérica Bidimensional da Queima de Partícula de Carvão em Atmosfera Oxidante O2/CO2 - Edital 20/2009". And also acknowledge the University of Brasilia, without which, this work could not have been undertaken.

8. REFERENCES

Abraham, B.M., Asbury, J.G., Lynch, E.P. and Teotia, A.P.S., 1982. In *Proceedings of the Oil & Gas Journal 80 (11), 68–70.*

Abbas, A.H., Naser, J. and Dodds, D., 2011. ―CFD modelling of air-fired and oxy-fuel combustion of lignite in a 100 KW furnace". In *Proceedings of the Fuel Jornal 90 (2011) 1778–1795*

Allam, R.J., White, V., Panesar, R.S. and Dillon, D., 2005. ―Optimising the design of an oxyfuel-fired advanced supercritical PF boiler". In *Proceedings of the 30th International Technical Conference on Coal Utilization & Fuel Systems. Coal Technology: Yesterday–Today–Tomorrow, April 17–21, Sakkestad, B.A. (ed).*

Atkinson, B. and Merrick D., 1982. ―Mathematical models of the thermal decomposition of coal". 4. Heat transfer and temperature profiles in a coke-oven charge. In *Proceedings of the National Coal Board, Coal Research Establishment, Stoke Orchard, Cheltenham, Glos., GL62 4RZ, UK.*

Bird, R.B., Stewart, W.E. and Lightfoot, E.N., 2001. *Transport Phenomena*. Second Edition, John Wiley & Sons. ISBN 0-471-41077-2.

Borman, G.L. and Ragland, K.W., 1998. *Combustion Engineering.* Department of Mechanical Engineering, University of Wisconsin-Madison.

Buhre, B.J.P., Elliott, L.K., Sheng, C.D., Gupta, R.P. and Wall, T.F., 2005. ―Oxy-fuel combustion technology for coal-fired power generation". In *Proceedings of the Energy and Combustion Science 31, 283–307.*

CEPAC, 2008 ―O que é sequestro de Carbono?" Centro de Excelência em Pesquisa sobre Armazenamento de Carbono. <http://www.pucrs.br/cepac/?p=sequestro_carbono>.

Croiset, E., Douglas, P.L. and Tan, Y., 2005. ―Coal oxyfuel combustion: a review". In *Proceedings of the 30th International Technical Conference on Coal Utilization & Fuel Systems—Clearwater Coal Conference Clearwater.*

Cunha, F.A., 2010. *Modelo matemático para estudo de processos reativos de partículas de carvão e biomassa*. Tese de Doutorado. Universidade de Brasília, Brasília.

ISSN 2176-5480

Curtiss, C.F. and Hirschfelder, J. O.: J. Chem. Phys., 17,550 (1949).

Hjärtstam, S., Andersson, K., Johnsson, F. and Leckner, B., 2009. "Combustion characteristics of lignite-fired oxy-fuel flames". In *Proceedings of the Fuel Jornal 88 (2009) 2216–2224.*

IEA, 2005. "International Energy Agency". 20 June, 2005 <http://www.iea-coal.co.uk/site/ieaccc/home/>.

IPCC, 2004. "Intergovernmental Panel on Climate Change". 27 Oct. 2004 <http://www.ipcc.ch/>.

Kiga, T., 2001. In *Proceedings in Miura, T. (ed) (Nova Science Publishers Inc, Huntington, NY), pp. 185–241.*

Krishna, R. and Wesselingh, J.A., 1997. "The Maxwell-Stefan approach to mass transfer". In *Proceedings of the Chemical Engineering Science, Vol. 52, No. 6, pp. 861-911, 1997*

Merrick, D., 1982. "Mathematical models of the thermal decomposition of coal". 2. Specific heats and heats of reaction. In *Proceedings of the National Coal Board, Coal Research Establishment, Stoke Orchard, Cheltenham, Glos., GL52 4RZ, UK.*

Nikolopoulos, N., Nikolopoulos, A., Karampinis, E., Grammelis, P. and Kakaras, E., 2011. "Numerical investigation of the oxy-fuel combustion in large scale boilers adopting the ECO-Scrub technology". In *Proceedings of the Fuel Jornal 90 (2011) 198–214.*

OXYCFB300, 2012. "El proyecto compostilla OXYCFB300" <http://compostillaproject.eu/>.

Patankar, S.V., 1980. *Numerical Heat Transfer and Fluid Flow.* Hemisphere-McGraw-Hill, Washington, DC.

Rojas A.F. and Barraza, J.M., "Efecto de las condiciones de desvolatilización de carbones pulverizados sobre las características físicas de carbonizados". In *Proceedings of the Revista Ingeniería e Investigación VOL. 27 No.1, Abril de 2007 (32-40).*

Santos, S., Haines, M. and Davison, J., 2006. "Challenges in the development of oxy-combustion technology for coal fired power plant". In *Proceedings of the 31st International Technical Conference on Coal Utilization & Fuel Systems, Sakkestad, B.A. (ed). (Coal Technology Association, Sheraton Sand Key, Clearwater, FL, USA), p. 1.*

Scheffknecht, G., Al-Makhadmeh, L., Schnell, U. and Maier, J., 2011. "Oxy-fuel coal combustion—A review of the current state-of-the-art". In *Proceedings of the International Journal of Greenhouse Gas Control 5S (2011).*

Tan, Y., Croiset, E. and Douglas, M.A., 2006. "Thambimuthu V. Combustion characteristics of coal in a mixture of oxygen and recycled flue gas". In *Proceedings of the Fuel, Volume 85, Issue 4, March 2006, Pages 507–512.*

Thunman, H., Niklasson, F., Johnsson, F. and Leckner, B., 2001. "Composition of Volatile Gases and Thermochemical Properties of Wood for Modeling of Fixed or Fluidized Beds". In *Proceedings of the Energy & Fuels 15, 1488-1497*

Tognotti, L., Longwell, J.P. and Sarofim, A.F., 1990. "The products of the high temperature oxidation of a single char particle in an electrodynamic balance". In *Proceedings of the Twenty-Third Symposium (International) on Combustion/The Combustion Institute, 1990/pp. 1207-1213.*

Turns, S.R., 2000. *An Introduction to Combustion.* Propulsion Engineering Research Center and Department or Mechanical and Nuclear Engineering, The Pennsylvania State University, 2nd edition.

Turns, S.R., 2004. *An Introduction to Combustion.* Mcgraw-Hill, USA.

Ulzama, M.T.S., 2007. *A Theoretical Analysis of Single Coal Particle Behavior during Spontaneous Devolatilization and Combustion*. Dissertation, Moradabad, India.

Viskanta, R., 2005. "Combustion and Heat Transfer in Inert Porous Media". In *Proceedings of the Handbook of Porous Media, 2ª ed, CRC Press: Taylor & Francis Group, Boca Raton.*

Wall, T., 2005. "Fundamentals of oxy-fuel combustion". In *Proceedings of the Inaugural Workshop of the Oxy-fuel Combustion Network, November 29–30 Cottbus, Germany.*

Wall T., Liu Y., Spero C., Elliott L., Khare S., Rathnam R., ZeenathalF., Moghtaderi B., Buhre B., Sheng C., Gupta R, Yamada T. and Makino K., Yu J., 2009. "An overview on oxyfuel coal combustion—State of the art research and technology development". In *Proceedings of the chemical engineering research and design 87 (2009) 1003–1016.*

Wall, T.F., 2007. "Combustion processes for carbon capture". In *Proceedings of the Combustion Institute , pp. 31–47*

Wall, T.F. and Yu, J., 2009. "Coal-fired oxy-fuel technology status and progress to deployment". In *Proceedings of the 34th International Conference on Coal Utilization and Fuel Systems, Clearwater.*

Warnatz, J., Maas, U. and Dibble, R.W., 2006. *Combustion.* Library of Congress Control Number: 2006927345, Verlag Berlin Heidelberg Germany, 4th Edition

Westbrook, C.K. and Dryer, F.C., 1984. "Chemical kinetic modeling of hydrocarbon combustion". In *Proceedings of the Energy and Combustion Science, 10, 1-57*

Whitaker, S., 2005. "Coupled, Nonlinear Mass Transfer and Heterogeneous Reaction in Porous Media". In *Proceedings of the Handbook of Porous Media, 2ª ed, CRC Press: Taylor & Francis Group, Boca Raton.*

White, C.M., Strazisar, B.R., Granite, E.J., Hoffman, J.S. and Pennline, H.W., 2003. In *Proceedings of the Journal of the Air & Waste Management Association, 53(6): 645–715.*

Ziemniczac, A. and da Silva, C.V., 2012. "Análise do processo de oxi-combustão de carvão pulverizado em um gerador de vapor usando CFD". In *Proceedings of the Vivências Revista Eletrônica de Extensão da URI Vol.8 N.14:p.48-64.*

9. RESPONSIBILITY NOTICE

The authors are the only ones responsible for the printed material included in this paper.